

The Molecular Behaviors of Pyridinium/Imidazolium Based Ionic Liquids and Toluene Binary Systems

Hong Chen, Zonghua Wang, Xianzhen Xu, Shida Gong, and Yu Zhou*

Shandong Sino-Japanese Center for Collaborative Research of Carbon Nanomaterials, College of Chemistry and Chemical Engineering, Instrumental Analysis Center of Qingdao University, Qingdao University, Qingdao 266071, China.

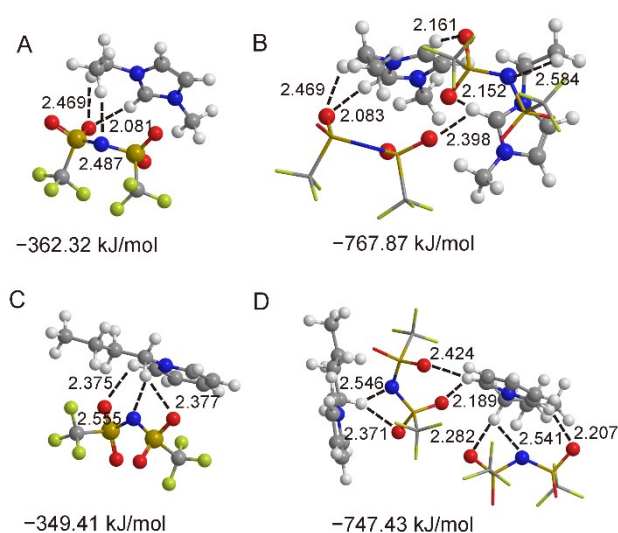


Fig. S1. The most stable optimized geometries for *trans*-EMIMTFSI (A), *trans*-2EMIMTFSI (B), *trans*-BpyTFSI (C), and *trans*-2BpyTFSI complexes (D). The interaction energies of each geometry was noted below the structure. Hydrogen bonds were denoted by dashed lines, and the corresponding distances of H \cdots O, H \cdots N and H \cdots F were labelled.

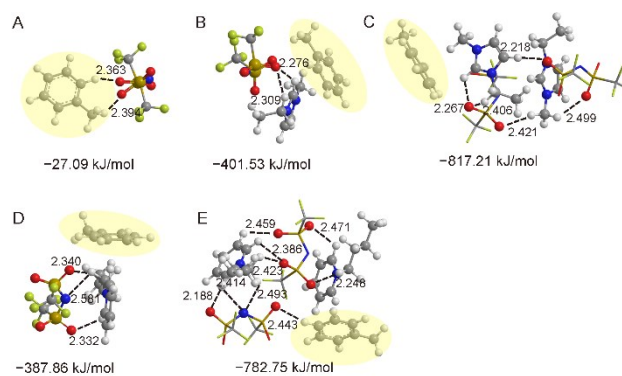


Fig. S2. The most stable optimized geometries for *trans*-[TFSI]⁻-C₆H₅CH₃ (A), *trans*-EMIMTFSI-C₆H₅CH₃ (B), *trans*-2EMIMTFSI-C₆H₅CH₃ (C), *trans*-BpyTFSI-C₆H₅CH₃ (D), and *trans*-2BpyTFSI-C₆H₅CH₃ (E) complexes. C₆H₅CH₃ was shown in a yellow shadow. For other information can be found in Fig. S1.

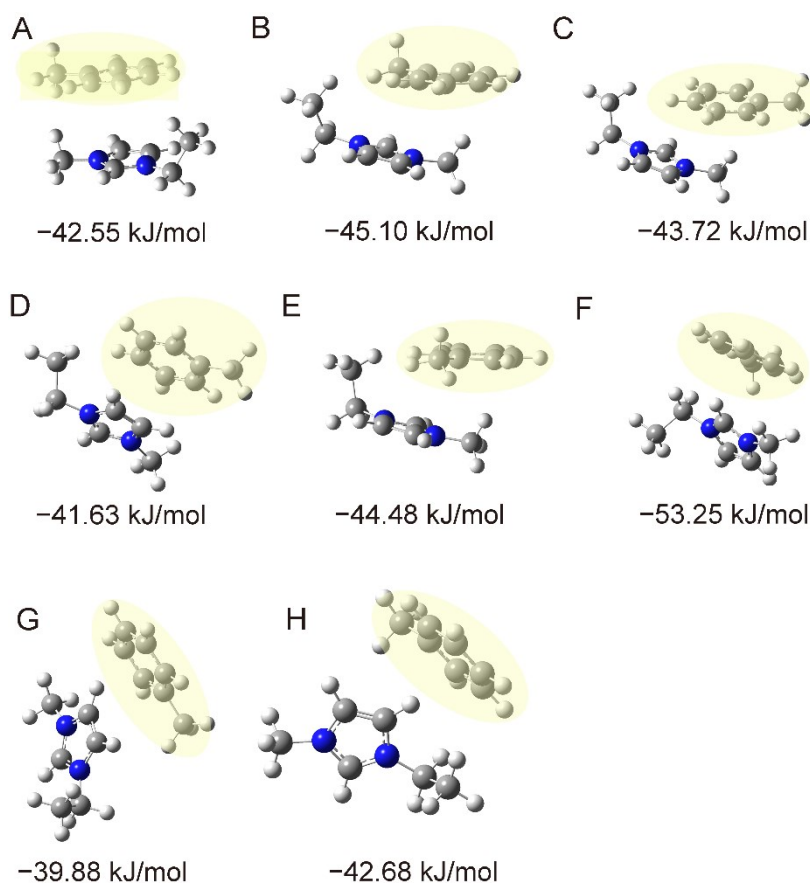


Fig. S3. The other stable optimized geometries for [EMIM]⁺-C₆H₅CH₃

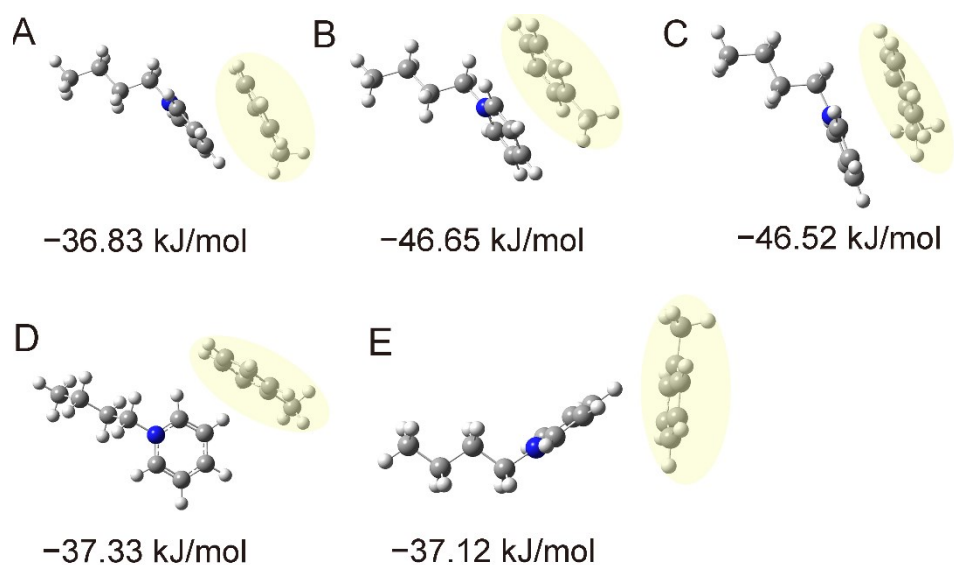


Fig. S4. The other stable optimized geometries for $[\text{Bpy}]^+-\text{C}_6\text{H}_5\text{CH}_3$

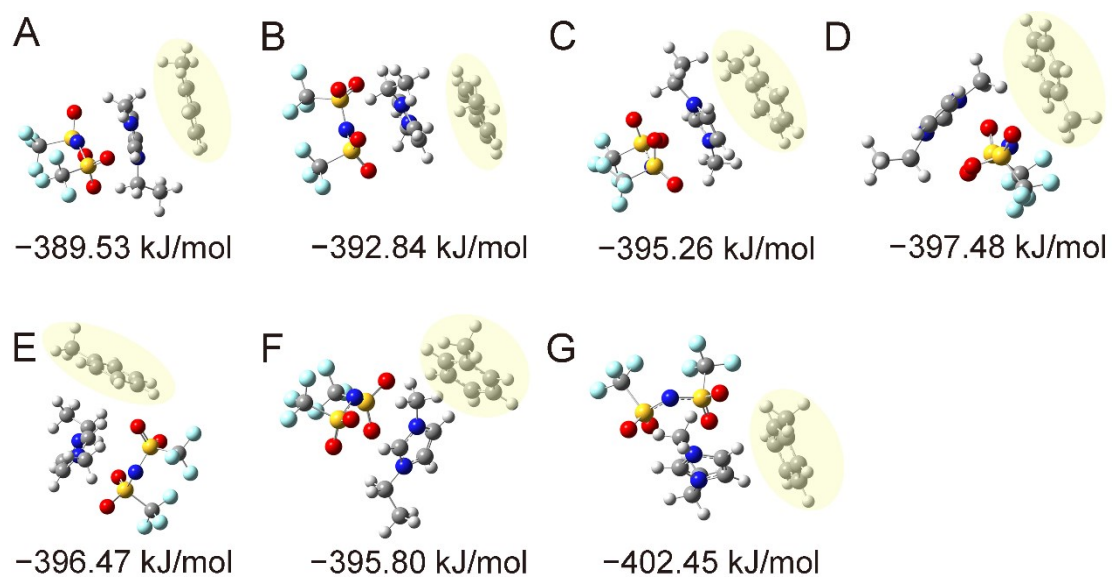


Fig. S5. The other stable optimized geometries for $\text{EMIMTFSI}-\text{C}_6\text{H}_5\text{CH}_3$

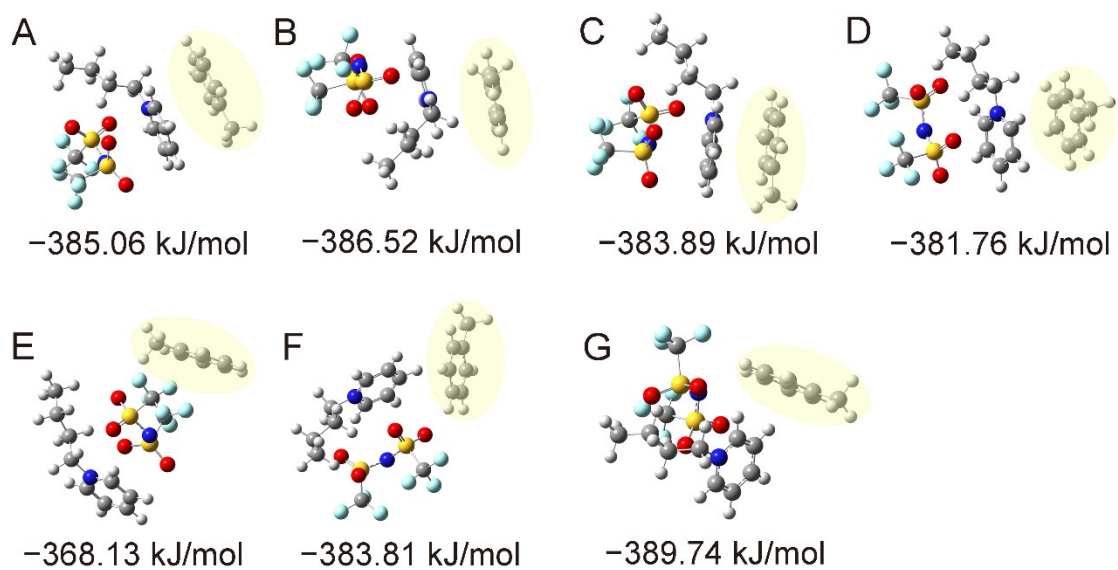


Figure S6. The other stable optimized geometries for BpyTFSI-C₆H₅CH₃

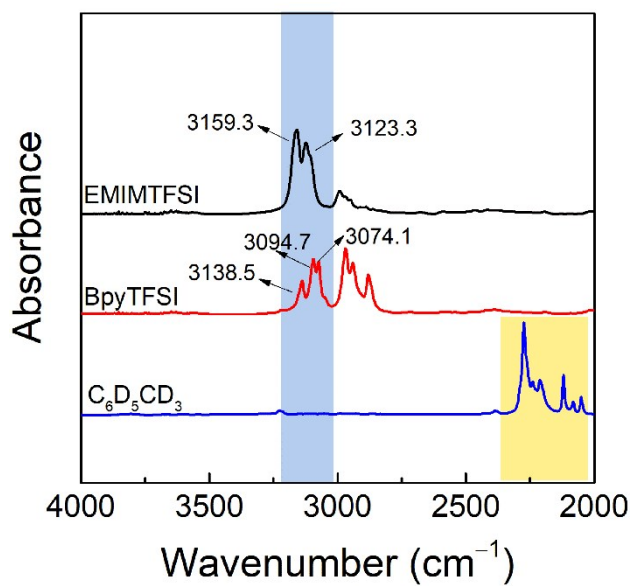


Fig. S7. ATR-FTIR spectra of pure EMIMTFSI, BpyTFSI, and C₆D₅CD₃ in the range of 4000–2000 cm⁻¹. The blue color region represents the main analysis region.

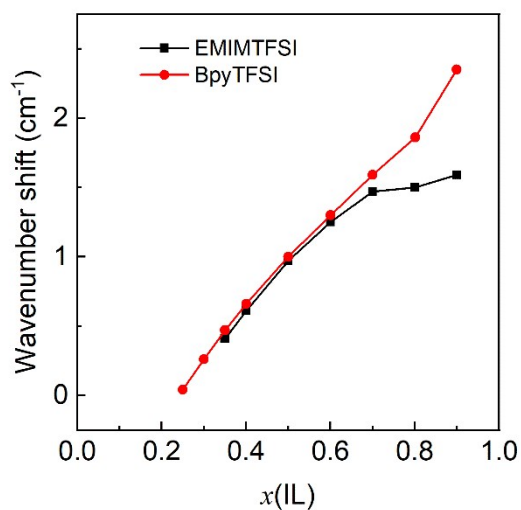


Fig. S8. Wavenumber shift of $\nu(\text{C-D})$ In the EMIMTFSI- $\text{C}_6\text{D}_5\text{CD}_3$ and BpyTFSI- $\text{C}_6\text{D}_5\text{CD}_3$ systems

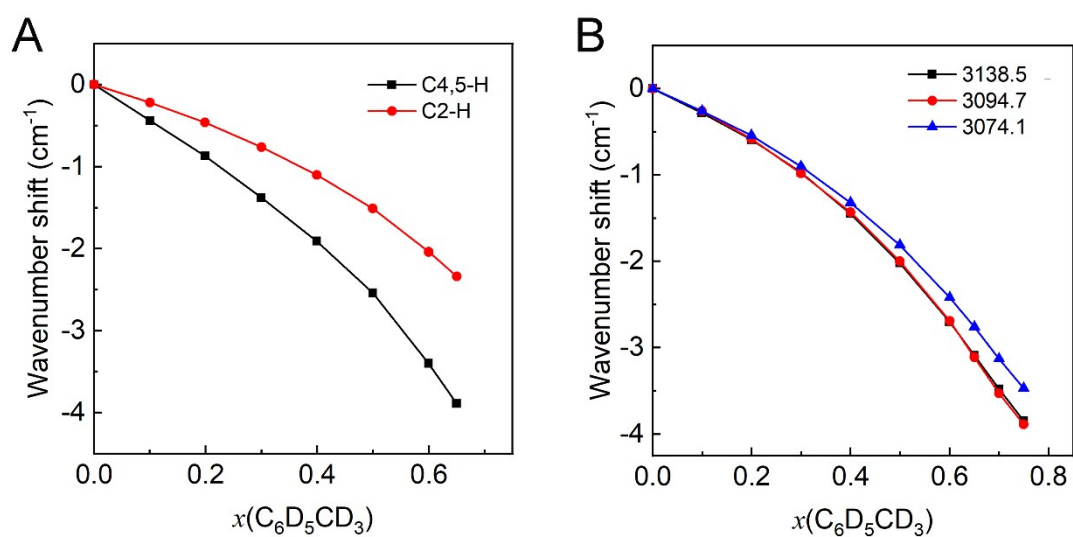


Fig. S9. Wavenumber shift of $\nu(\text{C-H})$ In the EMIMTFSI- $\text{C}_6\text{D}_5\text{CD}_3$ (A) and BpyTFSI- $\text{C}_6\text{D}_5\text{CD}_3$ (B) systems.